Journal of
Materials Chemistry B

Materials for biology and medicine

Accepted Manuscript

This article can be cited before page numbers have been issued, to do this please use: Q. Duan, G. Zheng, Z. Li, K. Chen, J. Zhang, L. Yang, Y. Jiang, H. Zhang, J. He and H. Sun, *J. Mater. Chem. B*, 2019, DOI: 10.1039/C9TB01279F.

This is an Accepted Manuscript, which has been through the Royal Society of Chemistry peer review process and has been accepted for publication.

Accepted Manuscripts are published online shortly after acceptance, before technical editing, formatting and proof reading. Using this free service, authors can make their results available to the community, in citable form, before we publish the edited article. We will replace this Accepted Manuscript with the edited and formatted Advance Article as soon as it is available.

You can find more information about Accepted Manuscripts in the Information for Authors.

Please note that technical editing may introduce minor changes to the text and/or graphics, which may alter content. The journal's standard Terms & Conditions and the Ethical guidelines still apply. In no event shall the Royal Society of Chemistry be held responsible for any errors or omissions in this Accepted Manuscript or any consequences arising from the use of any information it contains.

ROYAL SOCIETY OF CHEMISTRY

rsc.li/materials-b

View Article Online
DOI: 10.1039/C9TB01279F

ARTICLE

An ultra-sensitive ratiometric fluorescent probe for hypochlorite acid detection by the synergistic effect of AIE and TBET and its application of detecting exogenous/endogenous HOCl in living cells

Received 00th January 20xx,
Accepted 00th January 20xx

DOI: 10.1039/x0xx00000x

Qinya Duan,‡[a] Guansheng Zheng,‡[a] Zejun Li,‡[a] Ke Cheng,[b,c] Jie Zhang,[b,c] Liu Yang,[b,c] Yin Jiang,[a] Huatang Zhang,*[a] Jun He,*[a] and Hongyan Sun*[b,c]

An ultra-sensitive and ratiometric fluorescent probe for hypochlorite acid (HOCl) detection based on the mechanism of aggregation induced emission (AIE) and through-bond energy transfer (TBET) have been reported herein. By exploiting the advantages of AIE and TBET, which eliminates emission leakage from dark donors, the probe exhibits ultra-high sensitivity towards HOCl through an over 7000-fold fluorescence ratio enhancement ($I_{589\ nm}/I_{477\ nm}$), which is one of the highest records so far. The reaction mechanism has been discussed in detail, and the effects of interferent and the reaction of kinetic have also been investigated. Lastly, the successful result of exogenous/endogenous HOCl imaging detection in different cell lines indicates the potential use of the probe in living systems.

Introduction

Hypochlorite acid (HOCl) and its conjugate base (OCl^-) are important reactive oxygen species (ROS) and implicated in various physiological and pathological processes.[1-3] HOCl is produced endogenously through myeloperoxidase-catalyzed reaction of H_2O_2 and chloride ions.[4,5] Misregulation of HOCl is associated with various diseases such as cardiovascular diseases, neuron degeneration, diabetes and certain cancers.[6-11] There has been strong interest in the scientific community to investigate the roles of HOCl in biology and its link to the aforementioned diseases. Developing chemical methods for detecting HOCl will help to track HOCl in complex biological systems and further elucidate its biological roles.

Till date, numerous methods have been reported for quantitative measurements of HOCl, such as high-performance liquid chromatography, electrochemical methods and mass spectrometry. Nonetheless, these methods are not suitable for real-time detection of HOCl in living cells, tissue samples or animals. Fluorescence-based methods have recently emerged as a facile and attractive approach for detecting various bioanalytes. Compared with other approaches, fluorescence-based methods have several prominent advantages, such as high selectivity and sensitivity, non-invasive property and real-time monitoring capability.[12-18] During the past few years, a number of reaction-based fluorescence probes for HOCl detection have been developed by our group and others.[19-32] However, most of these probes are turn-on or turn-off probes. These probes are not ideal for live cell/animal imaging study because the fluorescence signal obtained is affected by numerous external factors, such as temperature, excitation power, medium characteristics, dye concentration as well as sensitivity of detector. On the other hand, ratiometric fluorescent probes, known as the third type of fluorescent probes, can effectively eliminate the limitations of surrounding environment. By utilizing self-calibration of two fluorescence emission intensities at different wavelengths, ratiometric fluorescent probes afford a built-in correction and thus exhibit superior application prospects over the other sensing mechanisms, namely turn-on probes and turn-off probes.[33-39] Consequently it is highly desired to develop novel ratiometric fluorescent probes to detect HOCl.

Although several fluorescent probes have been reported to detect HOCl with ratiometric property based on the mechanism of FRET or TBET,[40-48] most of the probes suffer from fluorescence leakage of the donor. This leads to low energy transfer efficiency even when the donors in the probe display high extinction coefficients and excellent quantum yields. Recently, Tang's group have developed new fluorescent probes based on the mechanism of dark through-bond energy transfer (DTBET).[49] The probes circumvented the emission leakage of the donor dyes, and the energy transfer efficiency can be improved to as high as 99%. Hence the background of the probe was dramatically reduced and the fluorescence ratiometric enhancement could be significantly improved. Our group have also reported a ratiometric fluorescent probe of Hg^{2+} based on the strategies of DTBET and aggregation-induced emission (AIE). The probe showed more than 30,000-fold ratiometric enhancement for Hg^{2+} detection.[50] Therefore, combining the mechanism of AIE and DTBET

[a] School of Chemical Engineering and Light Industry, Guangdong University of Technology, Guangzhou, Guangdong, 510006, China. E-mail: htzhang@gdut.edu.cn; junhe@gdut.edu.cn
[b] Department of Chemistry and Center of Super-Diamond and Advanced Films (COSDAF), City University of Hong Kong, 83 Tat Chee Avenue, Kowloon, Hong Kong, China. E-mail: hongysun@cityu.edu.hk
[c] Key Laboratory of Biochip Technology, Biotech and Health Centre, Shenzhen Research Institute of City University of Hong Kong, Shenzhen, 518057, China.
‡These authors contributed equally to this work.
†Electronic Supplementary Information (ESI) available: Synthesis, characterization, experimental details and supplementary figures. See DOI: 10.1039/x0xx00000x

View Article Online
DOI: 10.1039/C9TB01279F

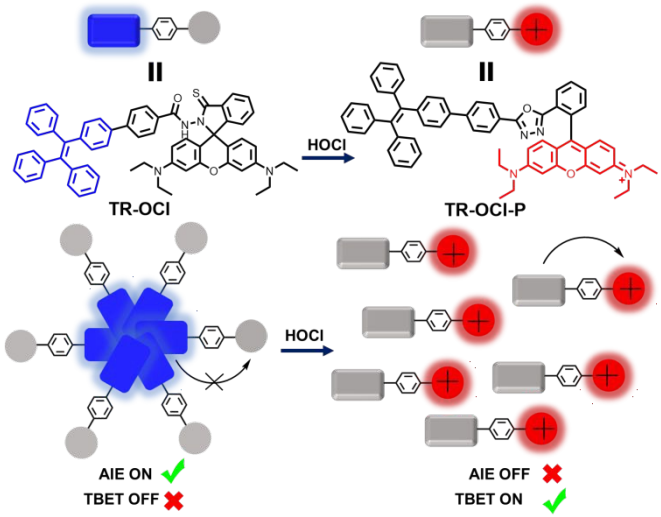

Scheme 1 Proposed reaction mechanism of **TR-OCl** with HOCl.

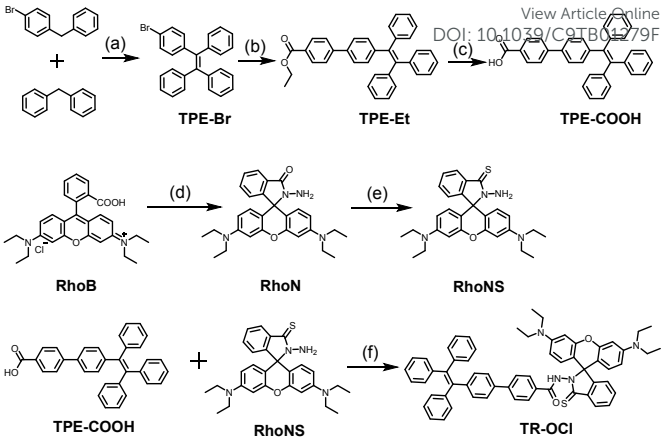

Scheme 2 The synthetic route for **TR-OCl**. (a) (i) n-BuLi, THF, (ii) *p*-TSA, toluene; (b) K_2CO_3, $Pd(PPh_3)_4$, Toluene/THF/H_2O, 110 °C, Ar; (c) NaOH, THF/H_2O, 90 °C, Ar; (d)NH_2-NH_2·H_2O, EtOH, 85 °C, reflux; (e) Lawesson's Reagent, Toluene, 110 °C, reflux, Ar; (f) (i) $SOCl_2$, DCM, (ii) Pyridine, 110 °C, Ar.

for constructing ratiometric fluorescent probes can yield ultra-high sensitivity compared with traditional ratiometric probes. Inspired by the above studies, we envisioned that based on DTBET and AIE strategy, we can design HOCl probe with high ratiometric fluorescence enhancement and improve the sensitivity of the current probes.

Herein, we report the design of an ultra-sensitive ratiometric fluorescent probe, **TR-HOCl**, for selective detection of HOCl in living cells. As depicted in Scheme 1, the probe consists of an energy transfer cassette, tetraphenylethene (TPE) and rhodamine B thiohydrazide (RBT). These two fluorophores play the roles of dark donor and acceptor respectively. In the absence of HOCl, the probe is in aggregated state and shows AIE property of blue emission from TPE. After reacting with HOCl, the rhodamine moiety becomes positively charged, resulting in enhanced solubility of the probe and no aggregation in water. Thus, emission from rhodamine can be observed due to the efficient DTBET process. In addition, due to the mechanism of DTBET, the dark donor of TPE does not leak any fluorescence emission, thus transferring its energy totally to the rhodamine moiety instead of exhibiting non-radiative decay. Our experimental results confirmed this synergistic effect and revealed a 7,000-fold fluorescence ratiometric enhancement, which is the highest recorded so far. In addition, **TR-OCl** demonstrates high kinetics as well as high selectivity. We also successfully applied **TR-OCl** to imaging exogenous/endogenous HOCl in different cells.

Experimental

TR-OCl was carried out in several steps with moderate yields in Scheme 2. Compounds TPE-Br, RhoN and RhoNS were synthesized as described previously by our groups and other groups.[50-52] Detailed information of synthesis and structure characterization with ^{1}H NMR, ^{13}C NMR and ESI-MS can be found in Supporting Information (see the ESI†).

Synthesis of TPE-Et. TPE-Br (822 mg, 2.0 mmol) was dissolved in a degassed mixture of solvents (THF/H_2O, 50 mL/20 mL). 4-ethoxycarbonylphenylboronic acid (427 mg, 2.2 mmol), K_2CO_3 (552 mg, 4.0 mmol) and $Pd(PPh_3)_4$ (232 mg, 0.2 mmol) were then added into the reaction flask under Ar atmosphere. The reaction was stirred at 110 °C overnight. The reaction progress was monitored with TLC till completion. The organic compound was extracted by dichloromethane from H_2O after THF was removed under vacuum. After removing dichloromethane under reduced pressure, the crude product was purified by column chromatography on silica gel (DCM/hexane=1/4, v/v) to give the compound TPE-Et (800 mg, 83%). ^{1}H NMR (400 MHz, $CDCl_3$) δ: 8.07 (d, *J* = 8.4 Hz, 2H), 7.61 (d, *J* = 8.4 Hz, 2H), 7.39 (d, *J* = 8.3 Hz, 2H), 7.09 (m, 17H), 4.40 (q, *J* = 7.1 Hz, 2H), 1.41 (t, *J* = 7.1 Hz, 3H); ^{13}C NMR (100 MHz, $CDCl_3$) δ: 166.67, 145.11, 143.90, 143.76, 143.73, 143.71, 141.61, 140.41, 137.77, 132.05, 131.52, 131.45, 130.11, 129.18, 127.94, 127.87, 127.79, 126.81, 126.74, 126.69, 126.64, 126.53, 61.07, 14.49.

Synthesis of TPE-COOH. TPE-Et (480 mg, 1.00 mmol) was dissolved in a degassed mixture of solvents (THF/H_2O, 10 mL/10 mL) firstly. NaOH (120 mg, 3.0 mmol) was then added into the reaction flask under Ar atmosphere. The resulting solution was stirred for 12 hours at 90 °C under Ar gas. The reaction progress was monitored with TLC till completion. The mixture was evaporated to remove THF and filtered to afford a crude solid product. The product was washed with water and dried in vacuo. The crude product was purified by column chromatography on silica gel (DCM/hexane=1/1, v/v) to give the compound TPE-COOH (360 mg, 80%). ^{1}H NMR (400 MHz, d^6-DMSO) δ: 7.98 (d, *J* = 8.2 Hz, 2H), 7.73 (d, *J* = 8.2 Hz, 2H), 7.52 (d, *J* = 8.1 Hz, 2H), 7.11 (m, 8H), 7.07 (d, *J* = 8.1 Hz, 2H), 7.00 (m, 7H); ^{13}C NMR (100 MHz, d^6-DMSO) δ: 167.62, 143.92, 143.72, 143.60, 143.55, 143.52, 141.51, 140.42, 137.19, 131.89, 131.20, 131.13, 131.11, 130.40, 130.08, 128.42, 128.36, 128.27, 127.20, 127.10, 127.06, 126.92, 126.68.

Synthesis of TR. TPE-COOH (226 mg, 0.5 mmol) was added into thionyl chloride (3 mL) in a reaction flask. The reaction was heated at 80 °C and kept stirring for 2 h. After the reaction completed, thionyl chloride was removed under reduced

pressure to give a white solid. RhoNS (228 mg, 0.5 mmol) was dissolved in dry pyridine (10 mL), and then the white solid was added to the reaction flask at room temperature under Ar atmosphere. The reaction solution was refluxed for 7 h. The solvent was removed under reduced pressure and the crude product was purified by column chromatography (DCM/hexane= 1/1, v/v) to give a pale-yellow solid (80 mg, 17%). ^{1}H NMR (400 MHz, d^6-DMSO) δ: 10.73 (s, 1H), 8.02 (d, J = 6.8 Hz, 1H), 7.62 (m, 6H), 7.50 (d, J = 8.3 Hz, 2H), 7.13 (m, 10H), 7.02 (m, 8H), 6.45 (d, J = 8.7 Hz, 2H), 6.32 (m, 4H), 3.26 (m, 8H), 1.07 (t, J = 6.9 Hz, 12H). ^{13}C NMR (100 MHz, d^6-DMSO) δ: 170.84, 164.50, 149.09, 143.62, 143.57, 143.55, 142.86, 141.44, 140.44, 137.25, 131.84, 131.74, 131.20, 131.12, 131.10, 130.17, 129.32, 128.94, 128.45, 128.37, 128.28, 127.21, 127.10, 127.05, 126.59, 108.11, 97.47, 60.23, 44.11, 21.24, 14.56, 12.90. ESI-MS m/z calcd. for: $[M+H]^+$: 907.40402 found 907.40363.

Results and discussion

Optical properties

After synthesis and characterization, preliminary optical properties tests of **TR-OCl** were carried out. Specifically, the AIE and DTBET properties of **TR-OCl** were investigated in a mixture of CH_3CN and water with different water fractions. Results showed that **TR-OCl** displayed emission from TPE moiety. The fluorescence intensity increased with over 40% water and reached a plateau at 60% water fraction (Fig. S1). After treating the probe with HOCl, the emission from TPE decreased whereas the emission from rhodamine moiety increased in the range of 0%-80% water fraction (Fig. S2). After systematically studying the ratio enhancement before and after the reaction with HOCl in different water fraction (Fig. S3), we selected CH_3CN/water=4/6 as the optimum testing condition for the following experiment.

We first measured the absorption and emission spectra of **TR-OCl** in the absence and presence of HOCl. As shown in Fig. 1, **TR-OCl** displays an absorption peak at 326 nm and an emission peak at 477 nm (TPE fluorescence). After the reaction with HOCl, a new absorption peak at 567 nm and an emission peak at 589 nm (Rhodamine fluorescence) appeared distinctly. In themeantime, the peaks of absorption and emission from TPE moiety decreased accordingly. It is noted that the emission intensity from TPE moiety has reduced significantly, indicating that the energy from dark TPE donor has transferred to rhodamine acceptor completely through TBET mechanism without fast non-radiative decay.

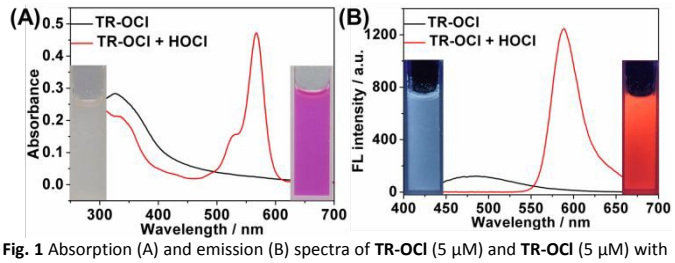

Fig. 1 Absorption (A) and emission (B) spectra of **TR-OCl** (5 μM) and **TR-OCl** (5 μM) with HOCl (100 μM) in the mixture of CH_3CN/H_2O (4/6, v/v). Inset pictures: photographs of colour (in A) and fluorescence changes (in B) in the absence and presence of HOCl.

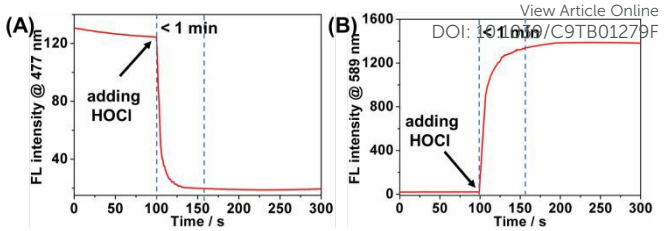

Fig. 2 Time-dependent fluorescence intensity of **TR-OCl** (5 μM) at 477 nm (A) and 589 nm (B) before and after the addition of HOCl in CH_3CN/H_2O (4/6, v/v).

The lifetime of HOCl is short in biological environment. Thus, it is important to investigate the detailed kinetics of our probe reacting with HOCl. A fast response of **TR-OCl** towards HOCl was observed (Fig. 2A and 2B). Specifically, the fluorescence intensity at 477 nm decreased and the fluorescence intensity at 589 nm increased significantly within one minute. In addition, the fluorescence intensities of **TR-OCl** and **TR-OCl-P** remained unchanged, indicating that both probes possess excellent stability. The fast response and the good stability of **TR-OCl** suggest that the probe is highly suited for real-time detection of HOCl in living cells.

Selectivity is another important factor to consider when designing HOCl probes. In a complex biological system, other reactive biomolecules can potentially react with the probe. To rule out these interferences, we performed detailed selectivity study with various reactive oxygen species (ROS) and reactive sulphide species (RSS), e.g. H_2O_2, ·OH, $ONOO^-$, $O_2^{\cdot-}$, Cys, Hcy and GSH. As shown in Fig. 3A and 3B, all the tested species, except HOCl, exhibited low ratiometric enhancement (I_{589}/I_{477}). Most species display TPE fluorescence and no rhodamine fluorescence, suggesting **TR-OCl** does not react with these species. It is noted that $ONOO^-$ could decrease the TPE fluorescence. However, no fluorescence from rhodamine was observed as well. The ratio enhancement of $ONOO^-$ is trivial compared with that of HOCl. Hence, we did not further investigate the reaction mechanism of **TR-OCl** with $ONOO^-$. These results together clearly demonstrated that **TR-OCl** can detect HOCl with high selectivity over other reactive species.

Subsequently, concentration-dependent fluorescence response of **TR-OCl** with HOCl was examined. As shown in Fig. 4A, the fluorescence intensity at 477 nm decreased gradually upon the addition of HOCl. In the meantime, a gradual increase of fluorescence signal at 589 nm was observed. The ratio of two emission band signal (I_{589}/I_{477}) also increased gradually. Over 7,000-fold fluorescence signal ratio can be detected when the concentration of HOCl is higher than 110 μM (Fig. 4B). This is the highest record achieved by ratiometric HOCl probe up to now (Table S1). It is noteworthy that

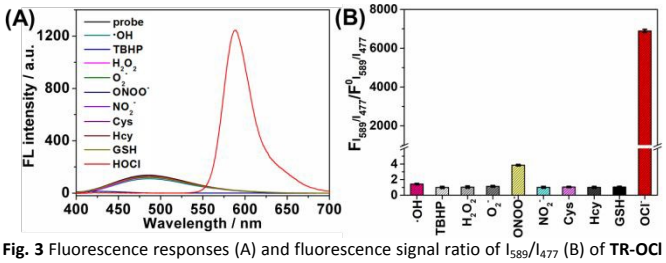

Fig. 3 Fluorescence responses (A) and fluorescence signal ratio of I_{589}/I_{477} (B) of **TR-OCl** (5 μM) towards various reaction species (100 μM) and HOCl (100 μM).

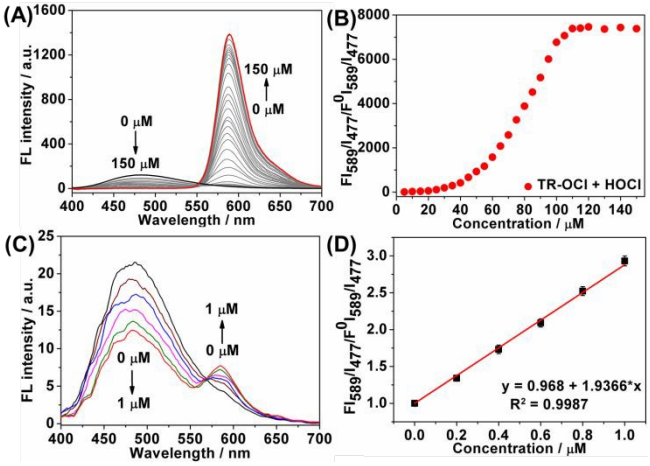

Fig. 4 (A) Fluorescence spectra of **TR-OCl** (5 μM) in the presence of different concentrations of HOCl (0-150 μM) (CH_3CN/H_2O=4/6, v/v); (B) Linearity between the fluorescent signal ratio and different concentrations of HOCl (0-150 uM), Incubation time: 1 min.; (C) Fluorescence spectra of **TR-OCl** (1 μM) in the presence of HOCl at low concentrations (0-1 μM) (CH_3CN/H_2O=4/6, v/v); (D) Linearity between the fluorescent ratio enhancement and different concentrations of HOCl (0-1 μM). Incubation time: 10 min.

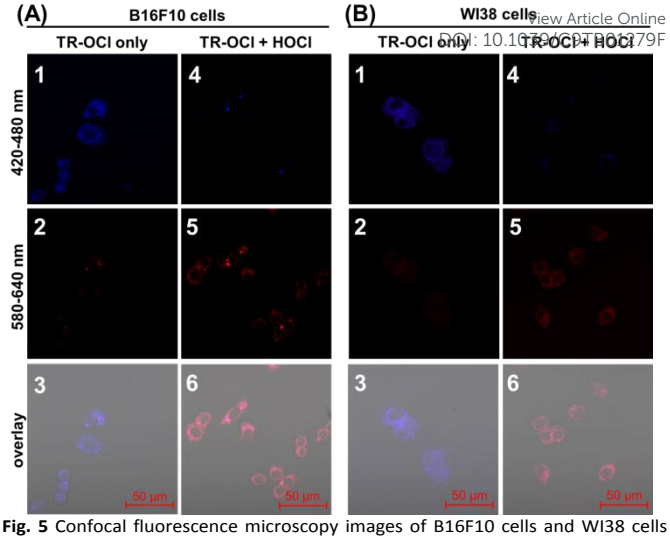

Fig. 5 Confocal fluorescence microscopy images of B16F10 cells and WI38 cells incubated with **TR-OCl** (25 μM) (A1-A3 and B1-B3) or **TR-OCl** (25 μM) for 2 h followed by 20 min of incubation with 50 μM HOCl (A4-A6 and B4-B6). blue channel: 420-480 nm, red channel: 580-640 nm.

TR-OCl also shows excellent reactivity when HOCl concentration is low. The reaction profile of low concentration HOCl is similar to that of high concentration HOCl (Fig. 4C & 4D). The fluorescence ratio enhancement with HOCl concentration in the range of 0-1000 nM can be fitted to the regression equation y = 0.968 + 1.9366 × x with R^2= 0.9987. The detection limit of HOCl is determined to be 1.29 nM based on the equation of 3σ/κ, where σ is the relative standard deviation of the blank measurements and κ is the slope between fluorescence ratio (I_{589}/I_{477}) versus HOCl concentration. The excellent linear relationship suggests that **TR-OCl** can be used as super-sensitive fluorescent probe for low concentration HOCl detection based on the DTBET mechanism.

Mechanism

We investigated the reaction mechanism of **TR-OCl** with HOCl. The plausible reaction mechanism is shown in Scheme 1. Before the reaction with HOCl, **TR-OCl** was hydrophobic and aggregated in CH_3CN/water=4/6, resulting in strong TPE emission only. After reacting with HOCl, **TR-OCl** transformed to **TR-OCl-P** by HOCl-mediated cyclization of the monothiol-bishydrazide to 1,2,4-oxadiazole, in which the spirolactam ring of rhodamine was opened and formed a positively charged rhodamine. Consequently, the solubility of **TR-OCl-P** increased and the TPE fluorescence diminished. Although the reaction intermediate could not be captured, the final compounds with similar reaction mechanism have been confirmed by our and other research groups by high-resolution mass technology and NMR spectra.[47, 53] We further performed high-resolution mass spectrometry analysis and dynamic laser scattering (DLS) experiments to examine our hypothesis as well as reported methods (Fig. S4-S6). Before the reaction, **TR-OCl** was a neutral molecule and showed a peak of $[M+H]^+$ at 907.40363. After reacting with HOCl, the major peak was shifted to 837.41735, which belonged to **TR-OCl-P** ($[M]^+$) carrying a positive charge (Fig. S4 and S5). For DLS measurement, the **TR-OCl** (5 μM) solution showed a mean diameter of 267 nm, proving the aggregation phenomenon of the probe. After reaction with Hg^{2+}, no nanoparticle was observed by DLS (Fig. S6). These results together unambiguously confirmed that the probe detects HOCl ratiometrically through DTBET process.

Exogenous HOCl detection in living cells

After carefully characterizing the selectivity and sensitivity property, we next applied **TR-OCl** to imaging HOCl in living cells. **TR-OCl,** which formed nano size due to aggregation in cells, was taken up by cells through endolysosome and released into cytosol. It is noted that the cellular environment is very different from aqueous buffer condition. Although our probe requires the usage of organic solvent in vitro, we think the probe may still function well in living cell imaging study as the crowding cellular environment alters the solvent property such as water dynamics and viscosity.[54] The similar result has been confirmed by some literatures.[49,55-57] Prior to the imaging experiment, we evaluated the cytotoxicity of **TR-OCl** by MTT assay using B16F10 cells and WI38 cells. Cytotoxicity experiments showed that 87% of B16F10 cells survived and 82% of WI38 cells survived after 24 h of incubation with **TR-OCl** (25 μM) (Fig. S7). These experiments proved that **TR-OCl** is of low cytotoxicity towards cultured cell lines.

Next, we carried out bioimaging experiments for exogenous HOCl detection. B16F10 and WI38 cells were incubated separately with **TR-OCl** (25 μM) at 37 °C for 2 h. HOCl was then added to cells and incubated for another 20 min before confocal images were taken. In the absence of HOCl, cells emitted strong blue fluorescence of TPE but little red fluorescence, indicatingthat **TR-OCl** is cell permeable (Fig. 5A1-5A2 and 5B1-5B2). In contrast, after addition of HOCl for 20 min, cells displayed fluorescence decrease in blue channel and concomitant enhancement in red channel, indicating that **TR-**

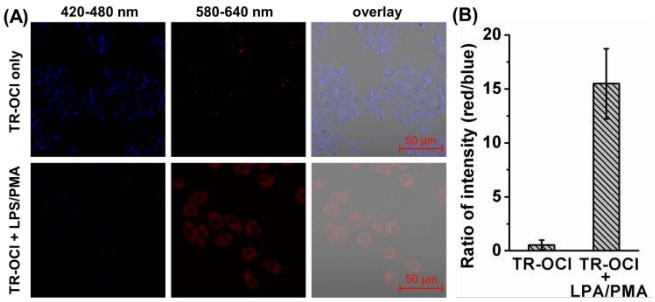

Fig. 6 (A) Confocal fluorescence microscopy images of RAW264.7 macrophages incubated with **TR-OCl** (25 μM) in the absence and presence of LPA (2 mg/mL)/PMA (2 mg/mL). (B) The ratio of fluorescence intensity (red/blue) changes from (A). Results are expressed as mean ± standard deviation of three independent experiments.

OCl reacted with HOCl and formed **TR-OCl-P** in the living cells (Fig. 5A4-5A5 and 5B4-5B5). The above fluorescence emission conversion from blue to red has clearly demonstrated that **TR-OCl** is capable of imaging HOCl in living cells.

Endogenous HOCl detection in RAW 264.7 macrophages

The literature reported that endogenous HOCl can be generated by stimulating the RAW 264.7 macrophages with LPS (lipopolysaccharide) and PMA (phorbol 12-myristate 13-acetate).[58-60] In our experiment, we investigated **TR-OCl** for imaging endogenous HOCl with the similar method. As shown in Fig. 6A, the RAW 264.7 macrophages treated with only **TR-OCl** showed obvious blue fluorescence and no red fluorescence. In contrast, after pretreating with LPS/PMA for 12 h and then **TR-OCl** at 37 °C for 2h, blue fluorescence darkened and red fluorescence remarkably increased. The corresponding ratio of red/blue were calculated from three cytosolic regions in the cells, which increased from 0.53 to 15.48, demonstrating that **TR-OCl** could monitor endogenous HOCl in living cells (Fig. 6B).

Conclusions

In summary, we have developed an ultra-sensitive ratiometric fluorescent probe, **TR-OCl**, to detect HOCl based on the synergistic effect of AIE and DEBET. The reaction mechanism has been discussed in detail and supported by DLS and mass spectrometry data. In addition, the effects of biological interferents and the stability of the probe and its reaction product have also been investigated in detail. Importantly, **TR-OCl** exhibits ultra-high sensitivity towards HOCl with 7,000-fold fluorescence ratio enhancement (I_{589}/I_{477}) and 1.29 nM detection limit, which is one of the highest records so far. Lastly, the successful application of **TR-OCl** to image exogenous/endogenous HOCl in different cell lines demonstrates the potential use of the probe in living systems.

Conflicts of interest

There are no conflicts to declare.

Acknowledgements

View Article Online
DOI: 10.1039/C9TB01279F

This work was supported by the National Natural Science Foundation of China (No. 21602033, 21807014 and 21702143), Guangxi Natural Science Foundation (2016GXNSFBA380123), the Pearl River Talent Plan of Guangdong Province (2017GC010596), Shenzhen Basic Research Project (JCYJ20180507181654823, JCYJ20160601173218804), the Hong Kong Research Grants Council (11213515) and the City University of Hong Kong grant (9667147).

References

1 T. Strowig, J. Henao-Mejia, E. Elinav and R. Flavell, *Nature* 2012, **481**, 278-286.
2 N. Branzk, A. Lubojemska, S. E. Hardison, Q. Wang, M. G. Gutierrez, G. D. Brown and V. Papayannopoulos, *Nat. Immunol.* 2014, **15**, 1017-1025.
3 G. Y. Liou and P. Storz, *Free Radical Res.*, 2010, **44**, 479-496.
4 M. J. Davies, *J. Clin. Biochem. Nutr.*, 2011, **48**, 8-19.
5 A. J. Kettle and C. C. Winterbourn, *Redox Rep.*, 1997, **3**, 3-15.
6 J. Perez-Vilar and R. C. Boucher, *Free Radical Bio. Med.*, 2004, **37**, 1564-1577.
7 S. Fu, M. J. Davies, R. Stocker and R. T. Dean, *Biochem. J.*, 1998, **333**, 519-525.
8 E. Malle, T. Buch and H. J. Grone, *Kidney Int.*, 2003, **64**, 1956-1967.
9 X. Chen, C. Guo and J. Kong, *Neural Regen. Res.*, 2012, **7**, 376-385.
10 S. A. Weitzman and L. I. Gordon, *Blood*, 1990, **76**, 655-663.
11 A. K. Yadav, A. Bracher, S. F. Doran, M. Leustik, G. L. Squadrito, E. M. Postlethwait and S. Matalon, *Proc. Am. Thorac. Soc.*, 2010, **7**, 278-283.
12 H.-W. Liu, L. Chen, C. Xu, Z. Li, H. Zhang, X.-B. Zhang and W. Tan, *Chem. Soc. Rev.*, 2018, **47**, 7140-7180.
13 L. Yuan, W. Lin, K. Zheng, L. He and W. Huan, *Chem. Soc. Rev.*, 2013, **42**, 622-661.
14 F. Yu, X. Han and L. Chen, *Chem. Commun.*, 2014, **50**, 12234-12249.
15 Z. Guo, S. Park, J. Yoon and I. Shin, *Chem. Soc. Rev.*, 2014, **43**, 16-29.
16 G. Niu, R. Zhang, J. P. C. Kwong, J. W. Y. Lam, C. Chen, J. Wang, Y. Chen, X. Feng, R. T. K. Kwok, H. H.-Y. Sung, I. D. Williams, M. R. J. Elsegood, J. Qu, C. Ma, K. S. Wong, X. Yu and B. Z. Tang, *Chem. Mater.*, 2018, **30**, 4778-4787.
17 X. Shi, C. Y. Y. Yu, H. Su, R. T. K. Kwok, M. Jiang, Z. He, J. W. Y. Lam and B. Z. Tang, *Chem. Sci.*, 2017, **8**, 7014-7024.
18 G. Niu, R. Zhang, Y. Gu, J. Wang, C. Ma, R. T. K. Kwok, J. W. Y. Lam, H. H.-Y. Sung, I. D. Williams, K. S. Wong, X. Yu and B. Z. Tang, *Biomaterial.*, 2019, **208**, 72-82.
19 D. Shi, S. Chen, B. Dong, Y. Zhan, C. Sheng, T. D. James and Y. Guo, *Chem. Sci.*, 2019, **10**, 3715-3722.
20 Q. X. Duan, P. Jia, Z. H. Zhuang, C. Y. Liu, X. Zhang, Z. K. Wang, W. L. Sheng, Z. L. Li, H. C. Zhu, B. C. Zhu and X. L. Zhang, *Anal. Chem.*, 2019, **91**, 2163-2168.
21 Q. Xu, K. A. Lee, S. Lee, K. M. Lee, W. J. Lee and J. Yoon, *J. Am. Chem. Soc.*, 2013, **135**, 9944-9949.
22 H. Zhu, J. L. Fan, J. Y. Wang, H. Y. Mu and X. J. Peng, *J. Am. Chem. Soc.*, 2014, **136**, 12820-12823.
23 W. Zhang, W. Liu, P. Li, J. Q. Kang, J. Y. Wang, H. Wang and B. Tang, *Chem. Commun.*, 2015, **51**, 10150-10153.
24 X. J. Jiao, C. Liu, Q. Wang, K. Huang, S. He, L. C. Zhao and X. S. Zeng, *Anal. Chim. Acta.*, 2017, **969**, 49-56.
25 Y. Koide, Y. Urano, K. Hanaoka, T. Terai and T. Nagano, *J. Am. Chem. Soc.*, 2011, **133**, 5680-5682.

26 X. L. Liu, Z. X. Tang, B. Song, H. Ma and J. L. Yuan, *J. Mater. Chem. B*, 2017, **5**, 2849-2855.
27 Y. Jiang, G. Zheng, Q. Duan, L. Yang, J. Zhang, H. Zhang, J. He, H. Sun and D. Ho, *Chem. Commun.*, 2018, **54**, 7967-7970.
28 J. J. Hu, N. K. Wong, M. Y. Lu, X. M. Chen, S. Ye, A. Q. Zhao, P. Gao, R. Y. T. Kao, J. G. Shen and D. Yang, *Chem. Sci.*, 2016, **7**, 2094-2099.
29 X. Wang, X. Wang, Y. Feng, M. Zhu, H. Yin, Q. Guo and X. Meng, *Dalton Trans.*, 2015, **44**, 6613-6619.
30 S. I. Reja, V. Bhalla, A. Sharma, G. Kaur and M. Kumar, *Chem. Commun.*, 2014, **50**, 11911-11914.
31 Y. Jiang, G. Zheng, N. Cai, H. Zhang, Y. Tan, M. Huang, Y. He, J. He and H. Sun, *Chem. Commun.*, 2017, **53**, 12349-12352.
32 C. Zhang, Q. Nie, I. Ismail, Z. Xi and L. Yi, *Chem. Commun.*, 2018, **54**, 3835-3838.
33 J. Zhang, X. Chai, X.-P. He, H.-J. Kim, J. Yoon and H. Tian, *Chem. Soc. Rev.*, 2019, **48**, 683-722.
34 X. Chen, F. Wang, J. Y. Hyun, T. Wei, J. Qiang, X. Ren, I. Shin and J. Yoon, *Chem. Soc. Rev.*, 2016, **45**, 2976-3016.
35 J. Fan, M. Hu, P. Zhan and X. Peng, *Chem. Soc. Rev.*, 2013, **42**, 29-43.
36 j. Zhou and H. Ma, *Chem. Sci.*, 2016, **7**, 6309-6315.
37 M. H. Lee, J. S. Kim and J. L. Sessle, *Chem. Soc. Rev.*, 2015, **44**, 4185-4191
38 X. Li, X. Gao, W. Shi and H. Ma, *Chem. Rev.*, 2014, **114**, 590-659.
39 M. Ren, K. Zhou, L. He and W. Lin, *J. Mater. Chem. B*, 2018, **4**, 1716-1733.
40 J. Liu, W. Bu and J. Shi, *Chem. Rev.*, 2017, **117**, 6160-6224.
41 L. Wu, I. C. Wu, C. C. DuFort, M. A. Carlson, X. Wu, L. Chen, C. T. Kuo, Y. L. Qin, J. B. Yu, S. R. Hingorani and D. T. Chiu, *J. Am. Chem. Soc.*, 2017, **139**, 6911-6918.
42 J. Kang, F. J. Huo, Y. K. Yue, Y. Wen, J. B. Chao, Y. B. Zhang and C. X. Yin, *Dyes Pigments*, 2017, **136**, 852-858.
43 X. Wang, L. Zhou, F. Qiang, F. Wang, R. Wang and C. Zhao, *Anal. Chim. Acta.*, 2016, **911**,114-120.
44 Z. Lou, P. Li, P. Song and K. Han, *Analyst*, 2013, **138**, 6291-6295.
45 J. Park, H. Kim, Y. Choi and Y. Kim, *Analyst*, 2013, **138**, 3368-3371.
46 Y. W. Jun, S. Sarkar, S. Singha, Y. J. Reo, H. R. Kim, J. J. Kim, Y.-T. Chang and K. H. Ahn, *Chem. Commun.*, 2017, **53**, 10800-10803.
47 L. Yuan, W. Lin, Y. Xie, B. Chen and J. Song, *Chem. Eur. J.*, 2012, 18, 2700-2706.
48 X. Wu, Z. Li, L. Yang, J. Han and S. Han, *Chem. Sci.*, 2013, **4**, 460-467.
49 Y. C. Chen, W. J. Zhang, Y. J. Cai, R. T. K. Kwok, Y. B. Hu, J. W. Y. Lam, X. G. Gu, Z. K. He, Z. Zhao, X. Y. Zheng, B. Chen, C. Gui and B. Z. Tang, *Chem. Sci.*, 2017, **8**, 2047-2055.
50 Y. Jiang, Q. Duan, G. Zheng, L. Yang, J. Zhang, Y. Wang, H. Zhang, J. He, H. Sun and D. Ho, *Analyst*, 2019, **144**, 1353-1360.
51 N. R. Chereddy, P. Nagaraju, M.V. N. Raju, V. R. Krishnaswamy, P. S. Korrapati, P. R. Bangal, V. J. Rao, *Biosens. Bioelectron.*, 2015, **68**, 749-756.
52 Y. Zhou, X. Y. You, Y. Fang, J. Y. Li, K. Liu and C. Yao, *Org. Biomol. Chem.*, 2010, **8**, 4819-4822.
53 Y.-R. Zhang, N. Meng, J.-Y. Miao and B.-X. Zhao, *Chem. Eur. J.*, 2015, **21**, 19058-19063.
54 M. Feig, I. Yu, P. Wang, G. Nawrocki, and Y. Sugita, *J. Phys. Chem. B.*, 2017, **121**, 8009-8025.
55 M. Ren, B. Deng, K. Zhou, X. Kong, J.-Y. Wang, G. Xu and W. Lin, *J. Mater. Chem. B*, 2016, **4**, 4739-4745.
56 Y.-R. Zhang, X.-P. Chen, J. Shao, J.-Y. Zhang, Q. Yuan, J.-Y. Miao and B.-X. Zhao, *Chem. Commun.*, 2014, **50**, 14241-14244.
57 Y. Liu, Z.-M. Zhao, J.-Y. Miao, B.-X. Zhao, *Anal. Chim. Acta.*, 2016, **921**, 77-83
58 H. D. Xiao, K. Xin, H. F. Dou, G. Yin, Y. W. Quan and R. Y. Wang, *Chem. Commun.*, 2015, **51**, 1442-1445
59 K. Schroder, P. J. Hertzog, T. Ravasi and D. A. Hume, *J. Leukocyte Biol.*, 2004, **75**, 163;
60 J. Michaelis, M. C. Vissers and C. C. Winterbourn, *Arch. Biochem. Biophys.*, 1992, **2**, 555-562.

View Article Online
DOI: 10.1039/C9TB01279F

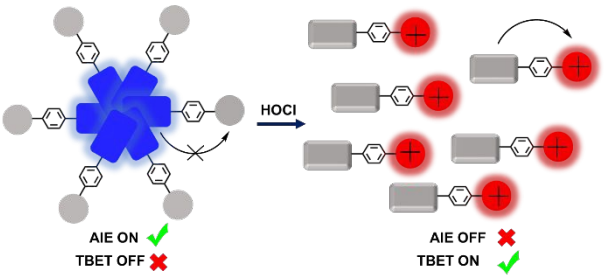

TR-OCl exhibits ultra-high sensitivity towards HOCl with 7,000-fold fluorescence ratio enhancement (I_{589}/I_{477}) and 1.29 nM detection limit, which is one of the highest records so far.